

Electronic supplementary information (ESI)

**†N, P, S co-doped hollow carbon polyhedron derived from
MOFs-based core-shell nanocomposites for capacitive
deionization**

Jing Zhang[‡], Jianhui Fang[‡], Jinlong Han, Tingting Yan, Liyi Shi and Dongsong Zhang*

Department of Chemistry, Research Center of Nano Science and Technology, Shanghai University,

Shanghai 200444, China.

E-mail: dszhang@shu.edu.cn

[‡]These authors contributed equally to this work.

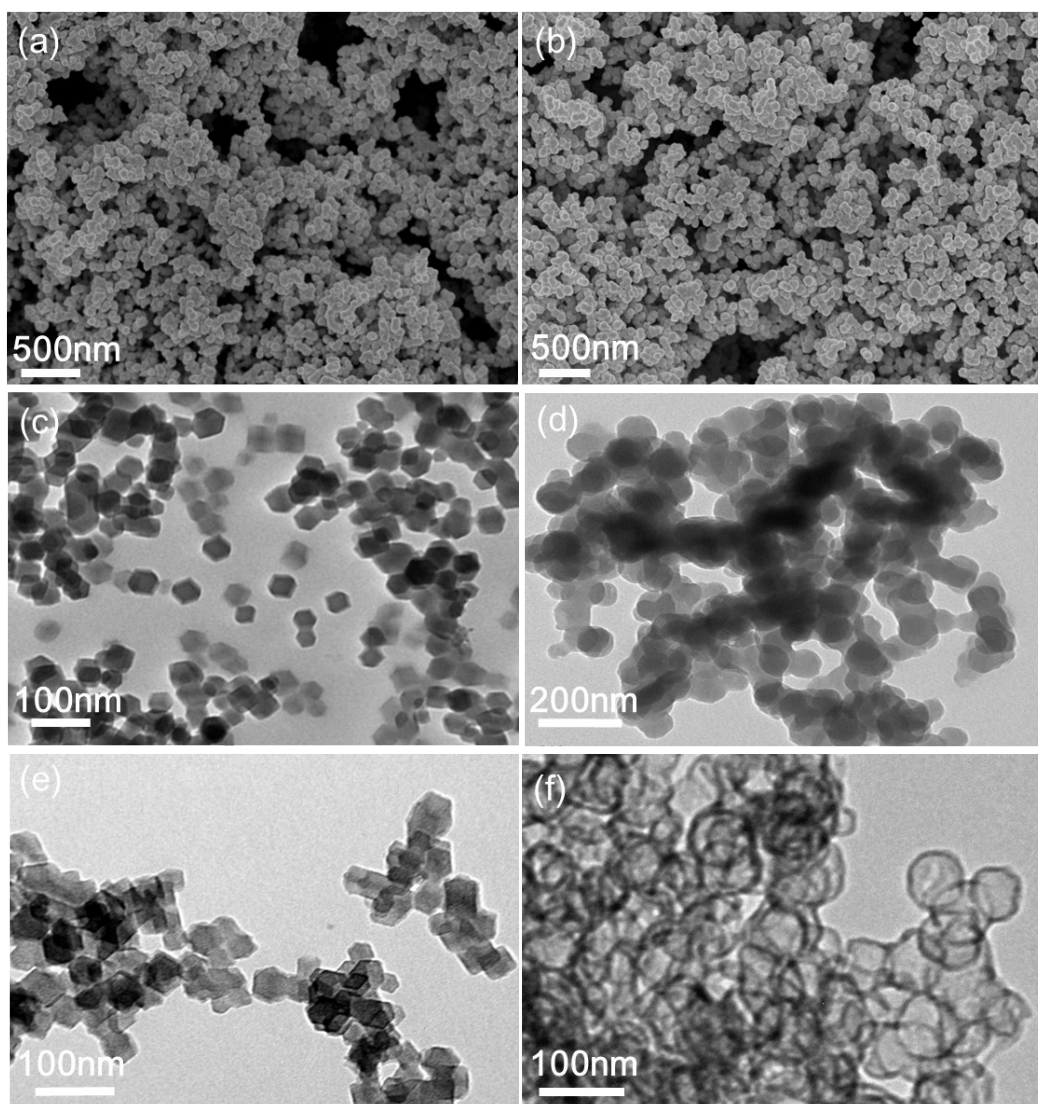


Fig. S1 (a and c) SEM images and TEM images of the prepared ZIF-8 polyhedrons. (b and d) SEM images and TEM images of the ZIF-8@PZS. (e and f) TEM images of the ZIF-8-C and the ZIF-8@PZS-C.

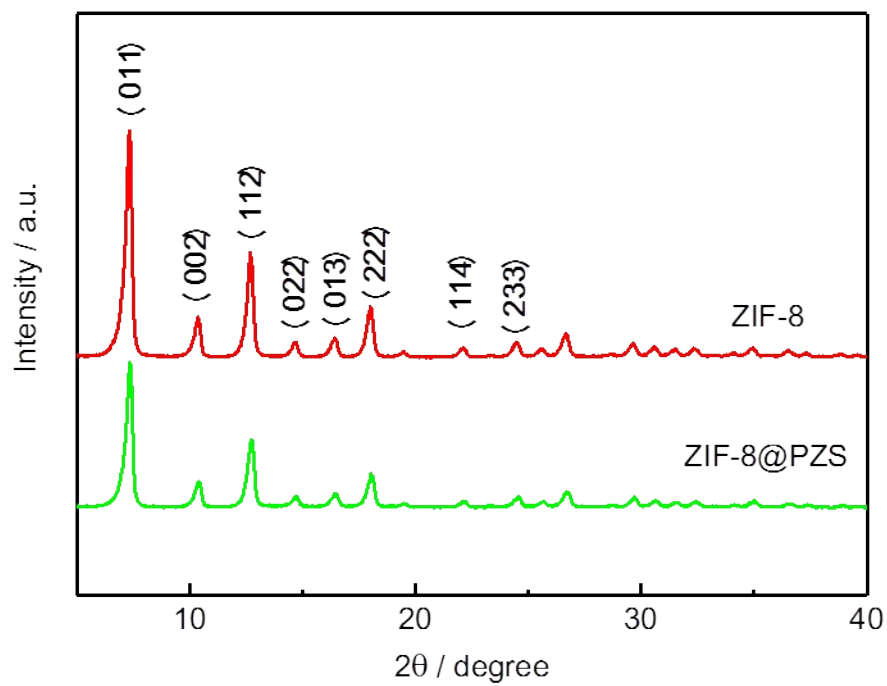


Fig. S2 XRD patterns of the normal ZIF-8 and ZIF-8@PZS.

As can be seen from Fig. S2, the XRD peaks of ZIF-8@PZS and ZIF-8 match very well, and the peak intensity of ZIF-8@PZS is lower, suggesting that ZIF-8@PZS is the pure crystalline phase.

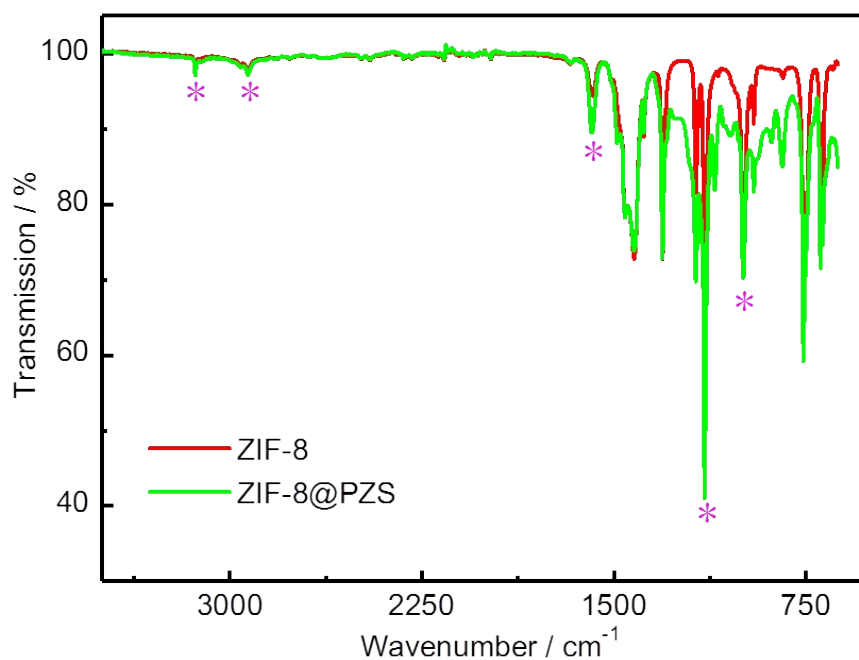


Fig. S3 FT-IR spectra of the normal ZIF-8 and ZIF-8@PZS.

As indicated in Fig. S3, the absorption peaks of ZIF-8 and ZIF-8@PZS exhibit typical IR bands, which are attributed to $\text{Zn}(\text{MeIm})_2$. The absorption peaks at around 3138 cm^{-1} and 2933 cm^{-1} are attributed to C-H stretching vibration modes in methyl and imidazole rings. The absorption peak at 1580 cm^{-1} are ascribed to C=N stretching vibration absorption. These broad bands at 1145 cm^{-1} and 990 cm^{-1} refer to the C-N stretching vibration modes. In addition, compared with ZIF-8, the peak intensity of ZIF-8@PZS is obviously enhanced. These results indicate the existence of PZS on the ZIF-8@PZS surface.

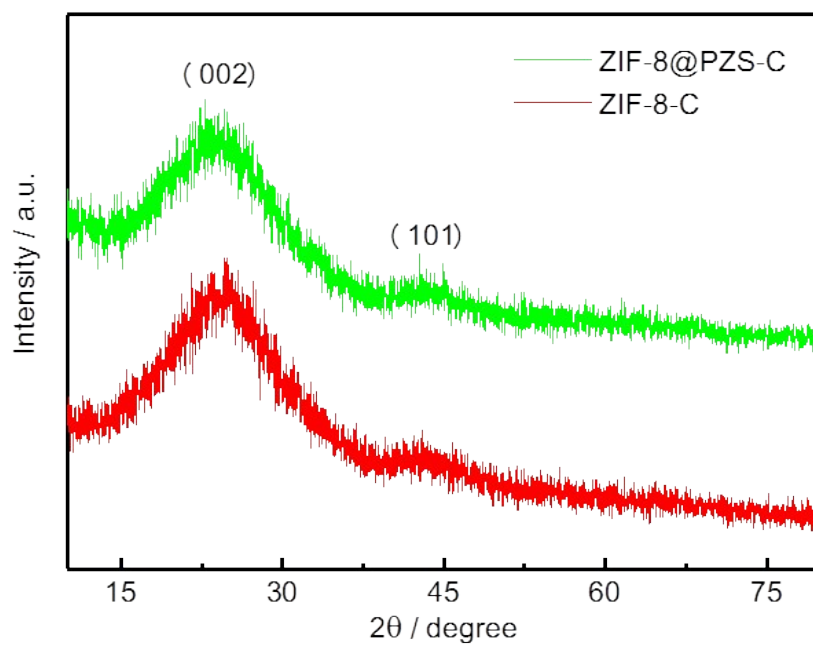


Fig. S4 XRD patterns of ZIF-8@PZS-C and ZIF-8-C.

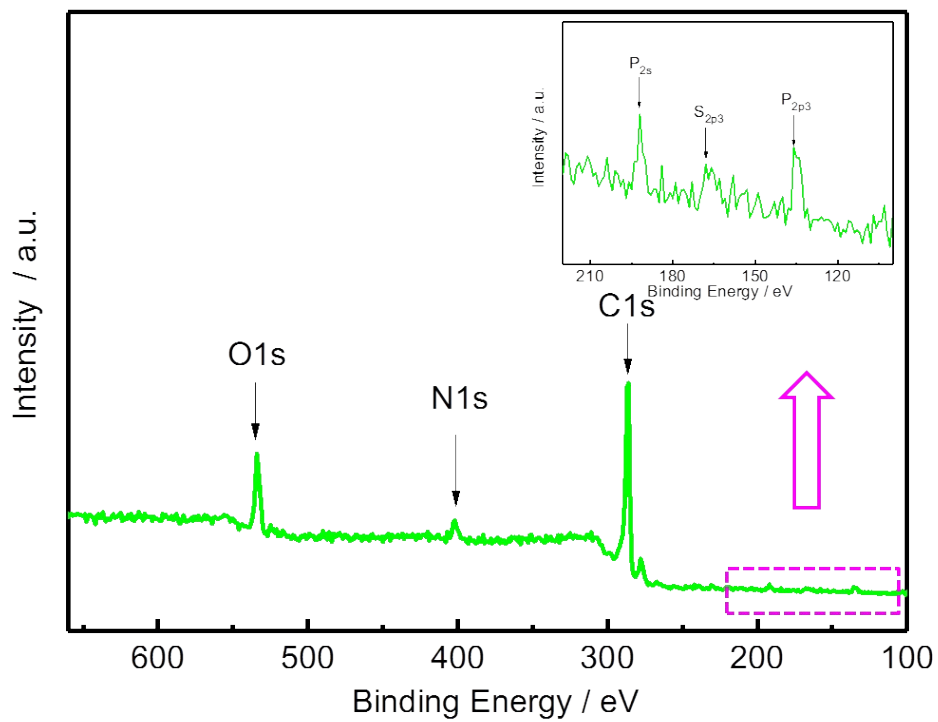


Fig. S5 Full XPS spectra of ZIF-8@PZS-C. The inset is the magnified area.

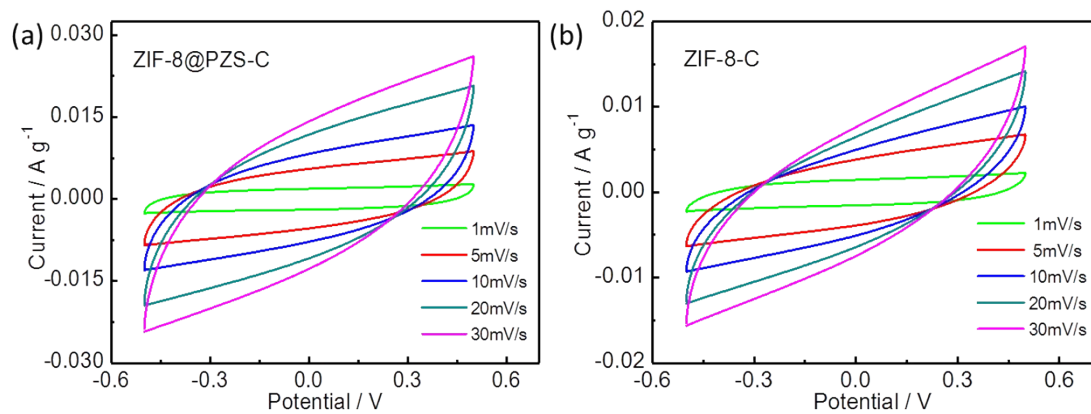


Fig. S6 Cyclic voltammograms of (a) ZIF-8@PZS-C and (b) ZIF-8-C electrodes at various scan rates. All the curves were obtained in a 0.5 M NaCl solution.

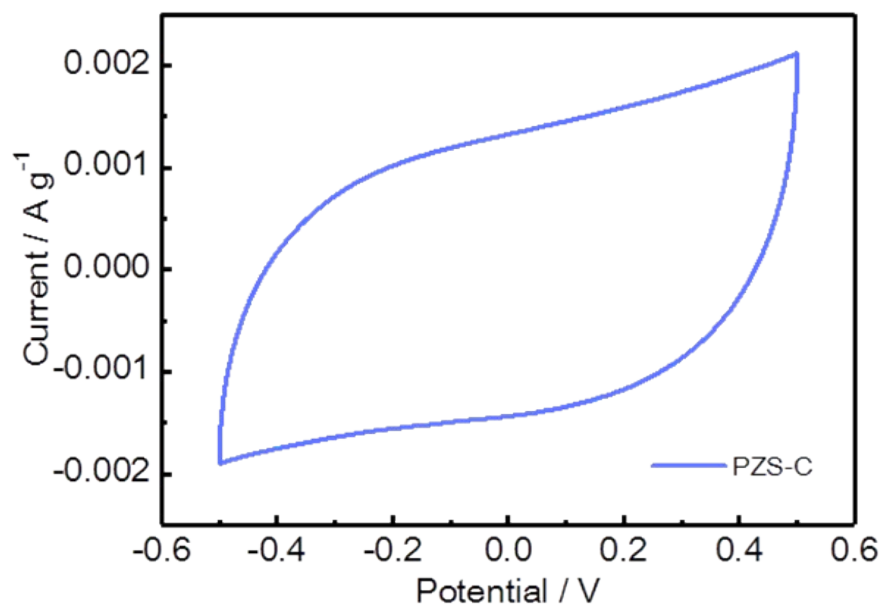


Fig. S7 Cyclic voltammograms of PZS-C at a scan rate of 1 mV s^{-1} . The curve was obtained in a 0.5 M NaCl solution.

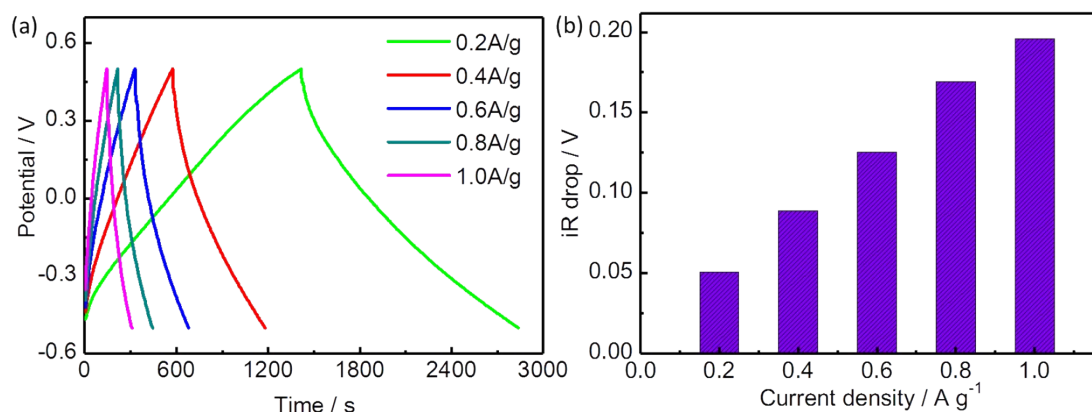


Fig. S8 (a) GCD curves at various current densities and (b) iR drop vs. current density of the ZIF-8@PZS-C electrodes. All the curves were obtained in a 0.5 M NaCl solution.

The iR drop decreases as the current density decreases. Theoretically, when the current density dropped to zero, the iR drop is also zero, and the voltage drop here is not zero because there is a certain error. The iR drop cannot be avoided completely. In a real electrochemical cell, the reference electrode is always located at a distance relative to the working electrode. This means that an additional resistance, called the uncompensated resistance (R_u), can never be avoided completely. The R_u leads to voltage fading across the electrochemical interface, called the iR drop. Therefore, whenever current is passed through the circuit, there is always a potential error due to R_u . Even with a very low R_u value, the voltage drop becomes significant when the current is high.

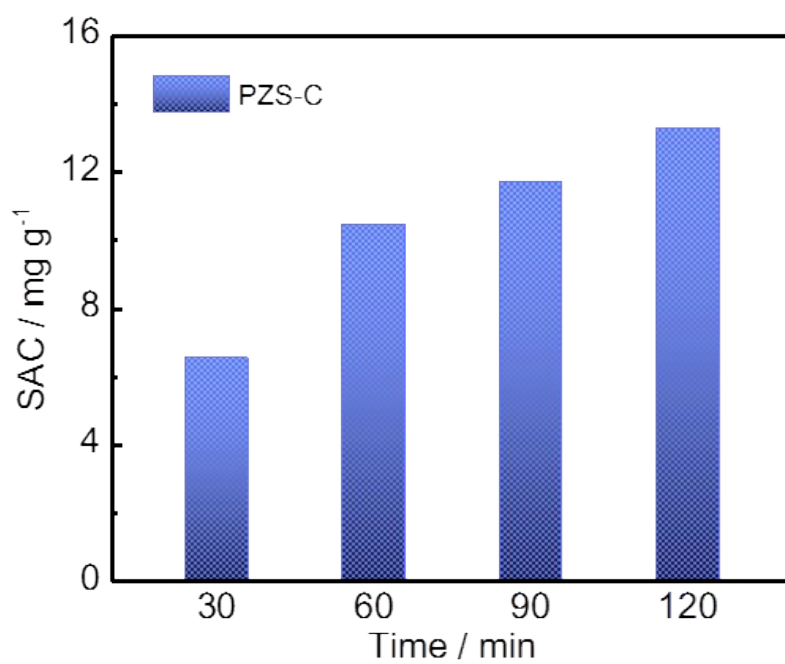


Fig. S9 Plots of SAC vs. deionization time of PZS-C electrodes in a 500 mg L^{-1} NaCl solution at

1.2 V with a flow rate of 50 mL min^{-1} .

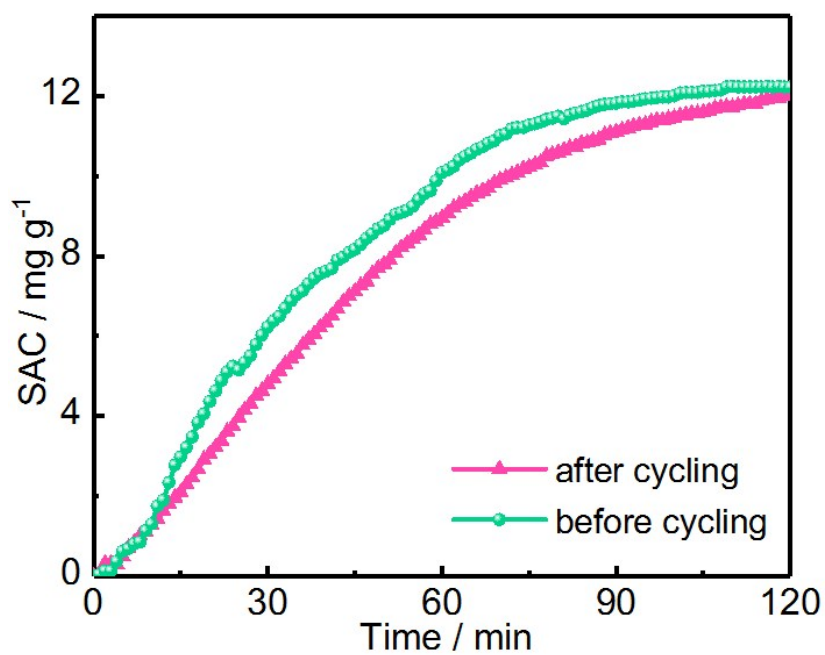


Fig. S10 Plots of SAC vs. desalination time at 1.2V in a 100 mg L⁻¹ NaCl solution with a flow rate of 50 mL min⁻¹ for the ZIF-8@PZS-C electrodes before and after cycling.

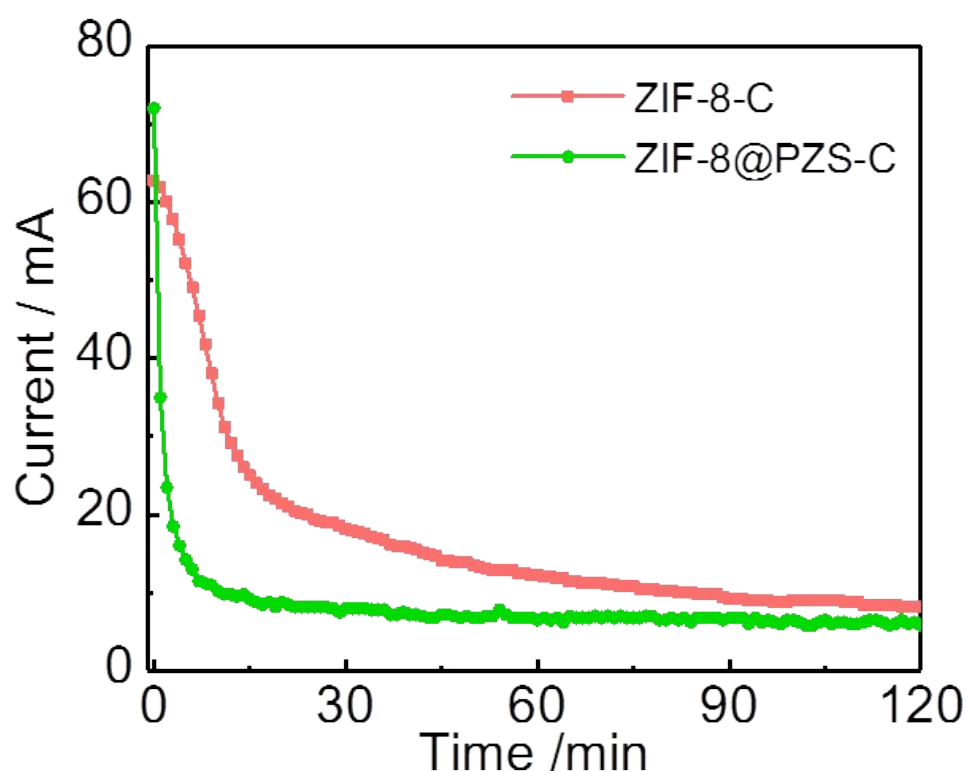


Fig. S11 Current transient curves and charge efficiency of ZIF-8@PZS-C and ZIF-8-C electrodes in a 500 mg L⁻¹ NaCl solution at 1.2 V with a flow rate of 50 mL min⁻¹.

It can be known from the results of EIS and *iR* drop analysis that the internal resistance of ZIF-8@PZS-C is smaller than that of ZIF-8-C. When the same voltage is applied between the two electrodes, ZIF-8@PZS-C has a higher initial current. Since ZIF-8@PZS-C is a hollow structure and has a certain proportion of mesopores compared to ZIF-8-C, salt ions are more likely to enter the hollow cavity and mesopores during salt adsorption. As the concentration of ion decrease, the current rapidly drops to a certain value. However, since ZIF-8-C has no hollow structure and few mesopores, the salt ion migration is slower and the current intensity decreases more slowly.

Table S1. Comparison of adsorption capacity of reported carbon materials.

Electrode materials	Applied voltage [V]	Initial NaCl concentration [mg L ⁻¹]	The mass of electrodes [g]	Adsorption capacity [mg g ⁻¹]	Ref.
Graphene Aerogels	1.2	500	0.20	9.9	1
N-doped porous carbon spheres	1.2	500	-	13.71	2
Porous carbon polyhedra	1.2	500	0.30	13.86	3
N-doped porous carbon	1.4	500	0.20	16.63	4
Micro/mesoporous carbon sheets	1.2	500	0.20	17.38	5
Carbon aerogel microsphere	1.2	500	0.85	5.62	6
Mesoporous carbons	1.2	250	0.19	4.8	7
3D graphene	1.2	500	0.20	14.7	8
N-doped porous hollow carbon spheres	1.4	500	0.20	12.95	9
Porous carbon	1.2	500	-	10.9	10
Porous graphene frameworks	1.4	500	0.16	19.1	11
ZIF-8@PZS-C	1.2	500	0.16	22.19	This work

Table S2. Surface Texture Properties of ZIF-8@PZS-C and ZIF-8-C.

Sample	S_{BET}	S_{micro}	$S_{\text{micro}}/S_{\text{BET}}$	V_{pore}	V_{micro}	$V_{\text{micro}}/V_{\text{pore}}$
	[$\text{m}^2 \text{g}^{-1}$]	[$\text{m}^2 \text{g}^{-1}$]	[%]	[$\text{cm}^3 \text{g}^{-1}$]	[$\text{cm}^3 \text{g}^{-1}$]	[%]
ZIF-8@PZS-C	929	530	57	1.60	0.22	13.75
ZIF-8-C	927	771	83	0.78	0.31	39.59

References

1. H. Yin, S. Zhao, J. Wan, H. Tang, L. Chang, L. He, H. Zhao, Y. Gao and Z. Tang, *Adv. Mater.*, 2013, **25**, 6270-6276.
2. Y. Liu, T. Chen, T. Lu, Z. Sun, D. H. C. Chua and L. Pan, *Electrochim. Acta*, 2015, **158**, 403-409.
3. Y. Liu, X. Xu, M. Wang, T. Lu, Z. Sun and L. Pan, *Chem. Commun.*, 2015, **51**, 12020-12023.
4. Z. Wang, T. Yan, J. Fang, L. Shi and D. Zhang, *J. Mater. Chem. A*, 2016, **4**, 10858-10868.
5. S. Zhao, T. Yan, Z. Wang, J. Zhang, L. Shi and D. Zhang, *RSC Adv.*, 2017, **7**, 4297-4305.
6. X. Quan, Z. Fu, L. Yuan, M. Zhong, R. Mi, X. Yang, Y. Yi and C. Wang, *RSC Adv.*, 2017, **7**, 35875-35882.
7. T. Gao, H. Li, F. Zhou, M. Gao, S. Liang and M. Luo, *Desalination*, 2017, DOI: 10.1016/j.desal.2017.06.021.
8. H. Wang, T. Yan, P. Liu, G. Chen, L. Shi, J. Zhang, Q. Zhong and D. Zhang, *J. Mater. Chem. A*, 2016, **4**, 4908-4919.
9. S. Zhao, T. Yan, H. Wang, G. Chen, L. Huang, J. Zhang, L. Shi and D. Zhang, *Appl. Surf. Sci.*, 2016, **369**, 460-469.
10. X. Duan, W. Liu and L. Chang, *J. Taiwan. Inst. Chem. E.*, 2016, **62**, 132-139.
11. H. Duan, T. Yan, G. Chen, J. Zhang, L. Shi and D. Zhang, *Chem. Commun.*, 2017, **53**, 7465-7468.